

## Facile Large-Scale Fabrication of Proton Conducting Channels

Basit Yameen,<sup>†</sup> Anke Kaltbeitzel,<sup>†</sup> Andreas Langner,<sup>‡</sup> Hatice Duran,<sup>†</sup> Frank Müller,<sup>‡</sup> Ulrich Gösele,<sup>‡</sup> Omar Azzaroni,<sup>\*,†,§</sup> and Wolfgang Knoll<sup>†</sup>

Max-Planck-Institut für Polymerforschung, Ackermannweg 10, 55128 Mainz, Germany, Max-Planck-Institut für Mikrostrukturphysik, Weinberg 2, 06120 Halle, Germany, and Instituto de Investigaciones Fisicoquímicas Teóricas y Aplicadas (INIFTA), Universidad Nacional de La Plata, CONICET, CC 16 Sucursal 4 (1900) La Plata, Argentina

Received June 19, 2008; E-mail: azzaroni@mpip-mainz.mpg.de; azzaroni@inifta.unlp.edu.ar

**Abstract:** A new approach to the facile large-scale fabrication of robust silicon membranes with artificial proton conducting channels is presented. Ordered two-dimensional macroporous silicon was rendered proton conducting by growing a thick uniform polyelectrolyte brush using surface-initiated atom transfer radical polymerization throughout the porous matrix. The fabricated silicon-poly(sulfopropyl methacrylate) hybrid membranes were evaluated for their proton conductivity, ion exchange capacity, and water uptake. With proton conductivities in the range of  $10^{-2}$  S/cm, these proof-of-concept experiments highlight a promising alternative for producing tailorable proton conducting membranes. This approach constitutes a benchmark for the preparation and study of model systems and, in addition, for the large-scale fabrication of membranes suitable for a wide range of technological applications.

### Introduction

Proton exchange membranes (PEMs) are key constituting elements in different industrial applications and particularly in energy conversion technologies.<sup>1,2</sup> To date, the PEMs are typically constituted of perfluorinated polyelectrolytes, like Nafion.<sup>3,4</sup> This material, considered “the golden standard”,<sup>5,6</sup> is characterized by forming nanoscopic hydrophilic channels suitable for the conduction of protons across the membrane, even if 60% of the hydrophilic domains at the surface of an operating Nafion membrane remain inactive.<sup>7</sup> The economical and environmental issues related to this material having moderate mechanical and chemical stability<sup>8</sup> represent serious drawbacks for the large-scale fabrication of cost-effective PEMs. In light of the current status,<sup>9</sup> it is clear that finding new technologies enabling the facile and low-cost production of efficient proton conducting platforms is a high priority goal, and it will constitute a tough scientific and technological challenge during the coming years. At present, the scientific community is actively exploring different strategies<sup>9</sup> including

the use of new chemistries to achieve perfluorinated polyelectrolytes,<sup>10</sup> development of polymeric membranes that could operate at higher temperatures without the need for humidification, for example, a phosphoric acid doped polybenzimidazole membrane,<sup>11</sup> or novel physicochemical approaches to tailor the proton transport like the use of porous substrates infiltrated with polyelectrolytes<sup>12</sup> and layer-by-layer polyelectrolyte films.<sup>13</sup>

On the other hand, the fabrication of self-standing macroporous ceramic membranes containing highly ordered and monodisperse channels is also attracting increasing interest.<sup>14</sup> In spite of their interesting architectures,<sup>15</sup> not much effort has been devoted to exploiting these channels to manipulate the proton conduction through the membrane. Here, we report an investigation on the use of ordered macroporous silicon modified with polyelectrolyte brushes for channelling the transport of protons that offers the potential of setting a new trend on the rational design of proton conducting membranes. We show that this strategy, combining elements from materials science and macromolecular chemistry,

<sup>†</sup> Max-Planck-Institut für Polymerforschung.

<sup>‡</sup> Max-Planck-Institut für Mikrostrukturphysik.

<sup>§</sup> Universidad Nacional de La Plata.

- (1) Jacobson, M. Z.; Colella, W. G.; Golden, D. M. *Science* **2005**, *308*, 1901–1905.
- (2) Steele, B. C. H.; Heinzel, A. *Nature* **2001**, *414*, 345–352.
- (3) Kreuer, K. D. *J. Membr. Sci.* **2001**, *185*, 29–39.
- (4) Kreuer, K. D.; Paddison, S. J.; Spohr, E.; Schuster, M. *Chem. Rev.* **2004**, *184*, 4637–4678.
- (5) Schmidt-Rohr, K.; Chen, Q. *Nat. Mater.* **2008**, *7*, 75.
- (6) Diat, O.; Gebel, G. *Nat. Mater.* **2008**, *7*, 13.
- (7) Bussian, D. A.; O’Dea, J. R.; Metiu, H.; Buratto, S. K. *Nano Lett.* **2007**, *7*, 227.
- (8) Kannan, R.; Kakade, B. A.; Pillai, K. *Angew. Chem., Int. Ed.* **2008**, *47*, 1–5.
- (9) Hickner, M. A.; Ghassemi, H.; Kim, Y. S.; Einsla, B. R.; McGrath, J. E. *Chem. Rev.* **2004**, *104*, 4587–4612.

- (10) Tsang, E. M. W.; Zhang, Z.; Shi, Z.; Soboleva, T.; Holdcroft, S. *J. Am. Chem. Soc.* **2007**, *129*, 15106–15107.
- (11) Wainright, J. S.; Wang, J. T.; Weng, D.; Savinell, R. F.; Litt, M. J. *Electrochem. Soc.* **1995**, *142*, L121–L123.
- (12) Yamaguchi, T.; Zhou, H.; Nakazawa, S.; Hara, N. *Adv. Mater.* **2007**, *19*, 592–596.
- (13) (a) DeLongchamp, D. M.; Hammond, P. T. *Langmuir* **2004**, *20*, 5403–5411. (b) DeLongchamp, D. M.; Hammond, P. T. *Chem. Mater.* **2003**, *15*, 1165–1173. (c) Lutkenhaus, J. L.; Hammond, P. T. *Soft Matter* **2007**, *3*, 804–816. (d) Argun, A. A.; Ashcraft, J. N.; Hammond, P. T. *Adv. Mater.* **2008**, *20*, 1539–1543.
- (14) Birner, A.; Wehrspohn, R. B.; Gösele, U.; Busch, K. *Adv. Mater.* **2001**, *13*, 377–388.
- (15) Fan, R.; Huh, S.; Yan, R.; Arnold, J.; Yang, P. *Nat. Mater.* **2008**, *7*, 303.

enables the robust and facile large-scale fabrication of artificial proton conducting channels.

## Experimental Section

**Materials and Methods.** (3-Aminopropyl)triethoxysilane 99%, 2-bromopropionyl bromide 97%, 2,2'-bipyridine 99%, copper(II) chloride,  $\text{CuCl}_2$ ,  $\geq 98\%$  (Fluka), and 3-sulfopropyl methacrylate potassium salt 98% were used as received from Sigma-Aldrich, Schnelldorf, Germany. Copper(I) chloride,  $\text{CuCl}$ ,  $\geq 97\%$  (Fluka) was purified by washing 5 times with glacial acetic acid. Sodium chloride 99.99% was obtained from Merck, Darmstadt, Germany. Triethylamine was refluxed overnight with calcium hydride before distilling and stored under argon. Dry dichloromethane was obtained from Acros organics, Geel, Belgium.  $^1\text{H}$  NMR was performed on a Bruker Spectrospin 250 MHz NMR spectrometer (Fallanden, Switzerland). Scanning electron microscopy (SEM) was performed with a LEO Gemini 1530 SEM. Atomic absorption spectroscopy (AAS) was performed on a Perkin-Elmer 5100 ZL spectrometer working in flame emission mode. The proton conductivity was measured by dielectric spectroscopy using either an Alpha high-resolution dielectric analyzer equipped with a Novocontrol active sample cell to expand the frequency range to  $\sim 10$  MHz or an SI 1260 impedance/gain-phase analyzer. XPS spectra were recorded on a VG ESCA Laboratory spectrometer using a monochromatic Al K $\alpha$  (1486 eV) irradiation source. Measurements were performed at a takeoff angle of  $45^\circ$  under Ultrahigh vacuum  $\sim 10^{-8}$  mbar. Data files were processed using the Unifit 2006 software package.

**Synthesis of Initiator (1) for SI-ATRP.** Two grams of (3-aminopropyl)triethoxysilane and 1.13 g of triethylamine in 40 mL of dry dichloromethane were mixed, stirred, and gradually cooled to  $0^\circ\text{C}$ . A 50% by volume solution of 2.56 g of 2-bromopropionyl bromide in dry dichloromethane was dropped in the reaction mixture over a period of 30 min, and the reaction mixture was allowed to stir at  $0^\circ\text{C}$  for 6 h under  $\text{N}_2(\text{g})$ . The reaction mixture was then filtered to remove the  $\text{Et}_3\text{N}^+\text{Br}^-$  salt precipitated during the reaction and residue was washed with small amount of dichloromethane. The filtrate was washed with brine ( $3 \times 25$  mL). The organic phase was dried over  $\text{MgSO}_4$ , and the solvent was removed *in vacuo* to yield 2-bromo-2-methyl-*N*-(3-triethoxysilyl-propyl)-propionamide **1** as a colorless oil-like liquid (yield = 66%).  $^1\text{H}$  NMR (250 MHz,  $\text{CDCl}_3$ ):  $\delta$  6.8 (1H, s), 3.76 (6H, q,  $J = 6.9$ ), 3.21 (2H, q,  $J = 6.6$  Hz), 1.88 (6H, s), 1.57 (2H, m), 1.16 (9H, t,  $J = 6.9$ ), 0.58 (2H, t,  $J = 8$  Hz).

**Anchoring 1 onto the Surface of Macroporous Silica and Subsequent PEB Growth by SI-ATRP.** The plasma-activated macroporous silica membranes were placed in a Schlenk tube containing 5  $\mu\text{L}$  of **1** in 10 mL of dry toluene at  $120^\circ\text{C}$  for 6 h under  $\text{N}_2(\text{g})$ . The membranes were then subjected to ultrasonication for 5 min each in toluene, ethanol, and THF. After drying with a stream of  $\text{N}_2(\text{g})$ , the membranes were stored under  $\text{N}_2(\text{g})$  until further use. Thick sulfonate PEB was grown on macroporous silica functionalized with **1**. The polymerization was carried out using aqueous ATRP as reported in literature:<sup>16</sup> 17.29 g of the sulfonate monomer (3-sulfopropylmethacrylate) was dissolved by stirring in 20 mL of methanol and 10 mL of water at room temperature. To this solution 0.651 g of BiPy and 0.0114 g of  $\text{Cu}(\text{II})\text{Cl}_2$  were added. The mixture was stirred and degassed by  $\text{N}_2(\text{g})$  bubbling for an hour before 0.1648 g of  $\text{Cu}(\text{I})\text{Cl}$  was added. The mixture was degassed with  $\text{N}_2(\text{g})$  bubbling for another 15 min. Initiator-coated macroporous silica samples were sealed in a Schlenk tube and degassed by four high vacuum pump/ $\text{N}_2(\text{g})$  refill cycles. The reaction mixture was syringed into this Schlenk tube, adding enough to cover the sample completely, and the mixture was left overnight under  $\text{N}_2(\text{g})$ . The samples were removed and thoroughly rinsed with deionized water. After the polymerization, the macroporous silica with PEB was extensively rinsed with water and kept overnight in

0.01N aq. HCl for exchanging the  $\text{K}^+$  ions that originally coordinated the monomer with  $\text{H}^+$ .

**Effective Loading by Weighing the Macroporous Silica Membrane after Each Step of Functionalization.** A 36.82 mg piece of the initiator-modified porous silicon membrane weighed 38.49 mg after growing the PEB by SI-ATRP followed by extensive washing with water, exchange of  $\text{K}^+$  counterions with  $\text{H}^+$ , drying with a stream of  $\text{N}_2$ , and overnight storage under vacuum at room temperature. The mass change reflected a 4.3% increase in weight during the functionalization of the membrane with the polyelectrolyte brush.

**Ion Exchange Capacity.** A 38.49 mg piece of porous silicon-PEB hybrid membrane in  $-\text{SO}_3\text{H}$  form was immersed in 15 mL of 2 mM solution of NaCl. After 24 h, the concentration of  $\text{Na}^+$  in the supernatant was reduced to 1.64 mM as determined by AAS. The ion exchange capacity of the membrane was calculated from eq 1 and was found to be 0.14 meq/g of the porous silica-PEB hybrid membrane.

$$IEC = \left( \frac{M_1 - M_2}{W} \right) \times V \quad (1)$$

$M_1$  and  $M_2$  are the molarities of the NaCl solution before and after immersing the porous silica-PEB hybrid membrane,  $W$  is the weight of the membrane, and  $V$  is the volume of the NaCl solution in which the porous silica-PEB hybrid membrane were immersed.

**Water Uptake Study.** Water uptake was measured gravimetrically. The porous silicon-PEB hybrid membrane was weighed after exposing to 100% relative humidity (RH) for 24 h ( $W_h$ ). Subsequently the membrane was allowed to dry first under ambient atmosphere (31% r.H.) followed by evacuating at  $50^\circ\text{C}$  for 2 h and weighed ( $W_{\text{dry}}$ ). The water uptake ( $WU$ ) of 7% ( $\pm 1\%$ ) was calculated from eq. 2.

$$WU = \left( \frac{W_h - W_{\text{dry}}}{W_h} \right) \times 100 \quad (2)$$

**Proton Conductivity Measurements.** The proton conductivity was measured by dielectric spectroscopy in a two-electrode geometry. The combination of high conductivity and thin sample can lead to distortions of impedance plots above 1 MHz. We have initially used an Alpha high-resolution dielectric analyzer and a Novocontrol active sample cell to expand the frequency range to  $\sim 10$  MHz. After proving that the resonance is below 1 MHz, the spectra were recorded using an SI 1260 impedance/gain-phase analyzer and a Novocontrol broadband dielectric converter. An atmosphere of saturated humidity was generated by using a closed sample cell with a water reservoir on the bottom that was not in contact with the sample. Saturation was controlled by a Sensirion SHT75 humidity sensor and found to be 100% (within the error bar of the sensor (2%)). Humidity between 18 and 95% was created using a temperature controlled climate chamber (Binder KBF 240). From the Cole–Cole and Bode plots, the resistance of the composite membrane was estimated, and then the specific conductivity of the composite membrane was calculated using the apparent thickness and electrode area.

## Results and Discussion

The macroporous silicon used in this study was grown by a photoelectrochemical etching process.<sup>17</sup> Subsequently, the remaining bulk silicon from the backside was removed in KOH and thus an ordered porous self-standing membrane<sup>14</sup> was obtained (Figure 1). The macroporous area conformed by perfectly parallel channels was  $\sim 3$  cm<sup>2</sup> with a density of  $\sim 10^7$  pores/cm<sup>2</sup>.

Next, we incorporated the proton source into the pore, that is, the polyelectrolyte. This was simply accomplished by surface-

(16) Ramstedt, M.; Cheng, N.; Azzaroni, O.; Mossialos, D.; Mathieu, H. J.; Huck, W. T. S. *Langmuir* **2007**, *23*, 3314–3321.

(17) Lehmann, V.; Föll, H. *J. Electrochem. Soc.* **1990**, *137*, 653.

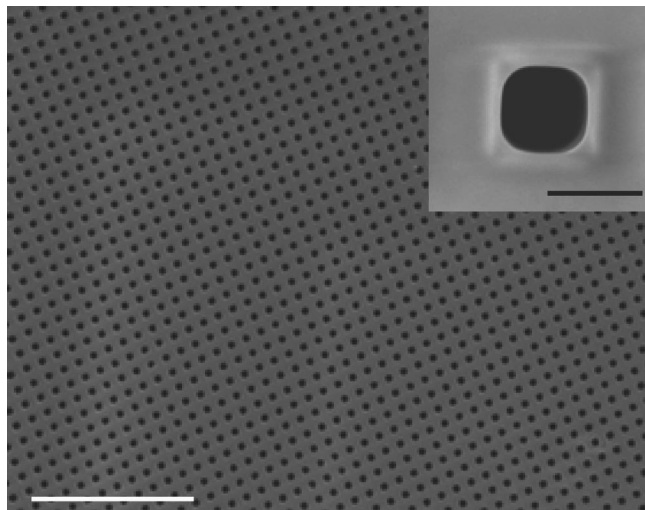


**Figure 1.** Scanning electron micrograph of the macroporous silicon membrane used as a platform for tethering the polyelectrolyte brush by surface-initiated atom transfer radical polymerization. Scale bar: 25  $\mu\text{m}$ . (Inset) Detail of the pore geometry. Scale bar: 800 nm.

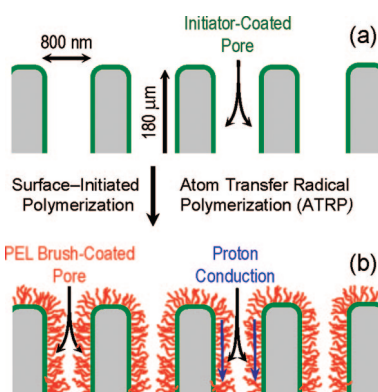


**Figure 2.** Simplified cartoon illustrating the construction of the polyelectrolyte brush-coated channels. The macroporous silicon membrane modified with initiator-terminated self-assembled monolayers (a) is immersed in the ATRP polymerization solution where the surface-initiated polyelectrolyte growth is carried out (b).

initiated atom transfer radical polymerization<sup>18</sup> (SI-ATRP). This polymerization process led to the formation of a dense polyelectrolyte layer (brush) covalently tethered at one end to the pore sidewall (Figure 2). Even if it is well-known that polymer brushes can be grown by a number of polymerization techniques,<sup>19</sup> ATRP<sup>20</sup> resulted in a very attractive alternative due to its simplicity to synthesize different polyelectrolytes (PELs) in aqueous environments.<sup>21</sup> First, we modified the macroporous substrate with initiator-terminated self-assembled monolayers (SAMs). To achieve this goal, we used 2-bromo-2-methyl-*N*-(3-triethoxysilyl-propyl)-propionamide monolayers assembled

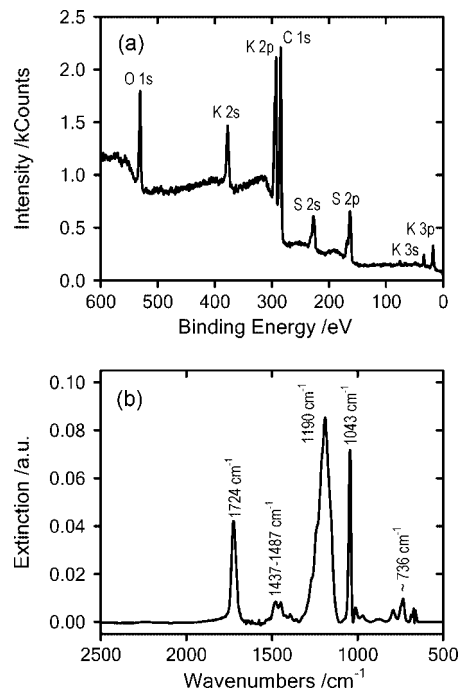


**Figure 3.** (a) XPS and (b) FTIR spectra corresponding to the substrate modification by surface-initiated polymerization of 3-sulfopropylmethacrylate. In panel (a), the signals correspond to carbon, C1s (284.5 eV); oxygen, O1s (531 eV); sulfur (from the sulfonate group), S2s (227.25 eV), S2p (163.25 eV); and potassium (monomer counterion), K2s (273.25 eV), K2p (293.75 eV) K3s (33.5 eV) K3p (17.5 eV). In panel (b), the spectrum shows the stretching of carbonyl groups at 1724  $\text{cm}^{-1}$ ,  $\text{CH}_2$  bending vibrations around 1437–1487 and 736  $\text{cm}^{-1}$ , and asymmetric and symmetric sulfonate stretching around 1190  $\text{cm}^{-1}$  and 1043  $\text{cm}^{-1}$ , respectively.

from toluene solutions. Second, we proceeded to the PEL brush growth (Figure 2) by immersing the initiator-modified macroporous substrates into the corresponding polymerization solution under conditions described elsewhere.<sup>16</sup>

The 3-sulfopropylmethacrylate monomer was chosen due to the fact that it is a simple and inexpensive sulfonated monomer. After polymerization, the chemical composition of the PEL brushes was monitored by XPS and FTIR. Both spectroscopic techniques corroborated that the chemical nature of the brush corresponded to poly(3-sulfopropylmethacrylate) coordinated with  $\text{K}^+$  ions (Figure 3). Then the brushes were extensively rinsed with water followed by dilute HCl for removing the  $\text{K}^+$  ions that originally coordinated the monomers.

The surface-initiated polymerization led to a homogeneous modification (Figure 4) of the silicon membrane resulting in a polymer layer evenly distributed on the porous substrate. Figure 4 clearly shows that the pore (mouth) diameter is significantly reduced after the polymer growth.

Cross-sectional analysis by scanning electron microscopy revealed that, in fact, the inner walls of the channels are uniformly and completely covered by  $\sim 200$  nm thick brushes (Figure 5), thus indicating that the SI-ATRP proceeded smoothly even in the confined environment of the macroporous silicon. On the other hand, polyelectrolyte brushes swell in humid environments leading to a significant increase in thickness.<sup>22</sup> This leads to fully occupied pores where the proton transport across the membrane is exclusively mediated by the hydronium ions through the polyelectrolyte brush.

(18) (a) Azzaroni, O.; Moya, S.; Farhan, T.; Brown, A. A.; Huck, W. T. S. *Macromolecules* **2005**, *38*, 10192–10199. (b) Farhan, T.; Azzaroni, O.; Huck, W. T. S. *Soft Matter* **2005**, *1*, 66–68. (c) Azzaroni, O.; Brown, A. A.; Huck, W. T. S. *Angew. Chem., Int. Ed.* **2006**, *45*, 1770–1774.

(19) Advincula, R. In *Surface-Initiated Polymerization I*; Jordan, R., Ed.; Springer-Verlag: Heidelberg, 2006; pp 107–136.

(20) Patten, T. E.; Xia, J.; Abernathy, T.; Matyjaszewski, K. *Science* **1996**, *272*, 866.

(21) (a) Cai, Y.; Armes, S. P. *Macromolecules* **2005**, *38*, 271–279. (b) Vo, C. D.; Schmid, A.; Armes, S. P.; Sakai, K.; Biggs, S. *Langmuir* **2007**, *23*, 408–413.

(22) Biesalski, M.; Ruhe, J. *Langmuir* **2000**, *16*, 1943–1950.

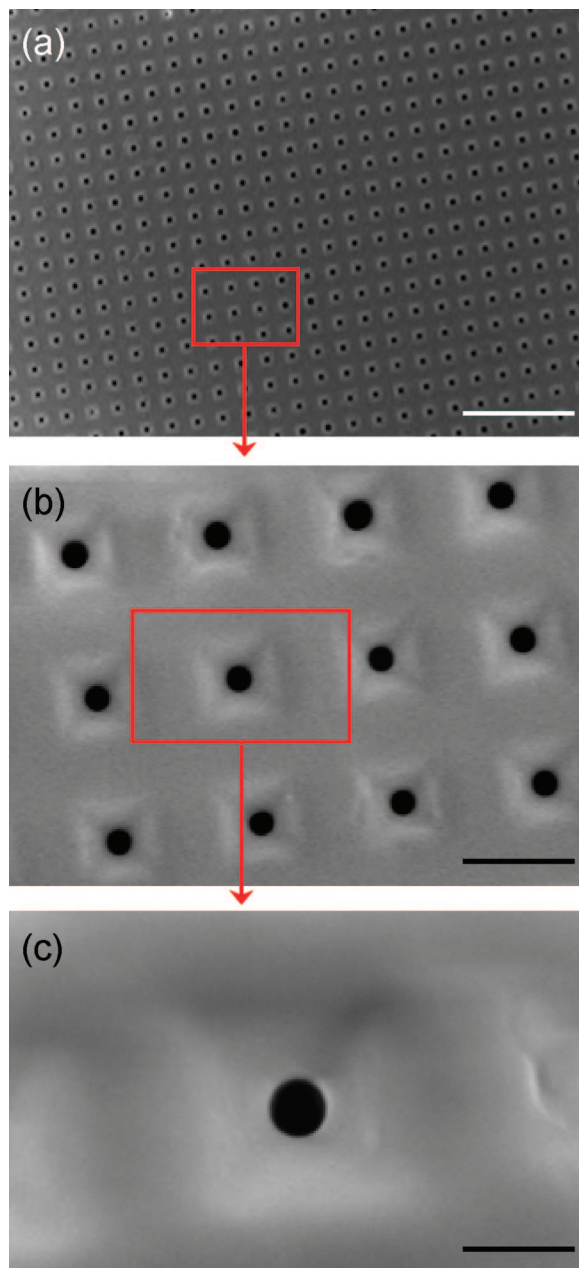


**Figure 4.** Scanning electron micrographs of the PEL brush-modified macroporous silicon membrane imaged at different magnifications. Scale bars are: (a) 12  $\mu\text{m}$ , (b) 2  $\mu\text{m}$ , (c) 600 nm.

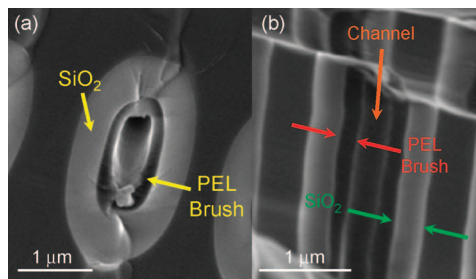


**Figure 5.** Scanning electron micrographs corresponding to: (a) cross-sectional imaging of a PEL brush-modified channel and (b) longitudinal cross-sectional imaging of the channel.

Once confirmed the modification of the channel wall with the brushes (Figure 5b), the effective loading (4.3%), the ion-

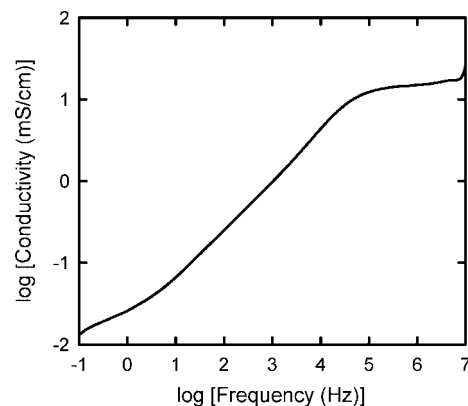


**Figure 6.** Bode plot describing the conducting characteristics of the polyelectrolyte brush-coated membrane at 100% RH and 25  $^{\circ}\text{C}$ . Evaluating the plateau of the Bode plot a specific conductivity of  $1.6 \times 10^{-2}$  S/cm was calculated.

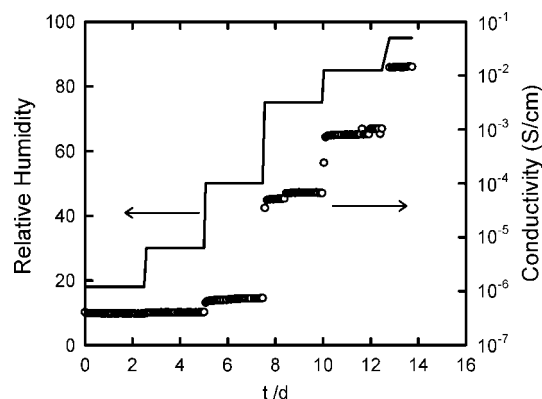


**Figure 7.** Variation of the proton conductivity with increase in RH. The different plateaus describe the stability displayed by the membrane at different preset RHs over the time in days. The membrane equilibrates quickly to the humidity changes and at each particular level of RH the proton conductivity was fairly constant over days.

exchange capacity (0.14 meq/g) and the water uptake (7%) of the self-standing membrane were estimated. The proton conductivity of the self-standing porous silicon-PEL brush hybrid membrane was measured using impedance spectroscopy. The impedance plot described in Figure 6 shows that in humidity saturated atmospheres the membrane displays conductivity values in the range of  $10^{-2}$  S/cm.

We have also studied the variations in proton conductivity of the polyelectrolyte brush-modified membrane upon changes in the RH at room temperature. A gradual increase in proton conductivity can be clearly observed upon increasing the RH (Figure 7). The proton conductivity at room temperature reaches the value of  $2 \times 10^{-2}$  S/cm at 95% RH. Importantly, the membrane quickly equilibrates to humidity changes and at each RH the proton conductivity was fairly constant over days (Figure 7), thus evidencing the good proton conducting characteristics of the PEL brush-modified macroporous silicon membrane. This approach provides a robust and highly reproducible strategy to firmly anchoring the PEL layer into the channels. This is a major improvement with respect to other methods based on polyelectrolyte impregnation into porous substrates<sup>12</sup> where humid environments lead to the continuous leaching of the polymer (proton source) and, consequently, to a significant decrease in the proton conductivity. In our case, the chemical nature of the

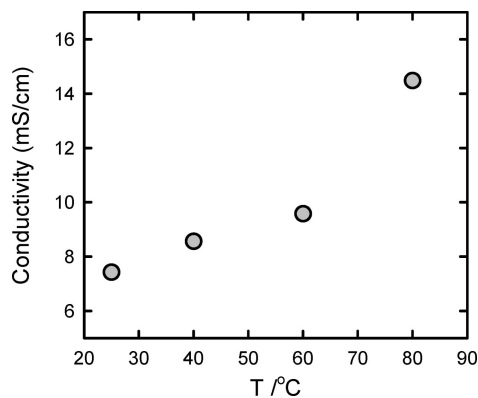


**Figure 8.** Conductivity versus temperature plot measured at RH 90% using a climate chamber.

silane linkage<sup>23</sup> enables the use of the PEL brushes in different environments<sup>24</sup> without affecting the stability of the anchoring layer. The simplicity of the procedure described here is also advantageous when compared to bulk copolymer-based PEMs, which require tedious synthetic routes to achieve proton conducting nanochannels.

To further investigate the characteristics of the platform, the porous silicon-(sulfopropyl methacrylate) hybrid membrane was subjected to temperature dependent proton conductivity measurements under highly humidified environments. At 90% RH, varying the temperature from 25 to 80 °C leads to an increase in proton conductivity from 7 to 15 mS/cm (Figure 8). These values further evidence the good proton conductivity performance of this approach when the platform is operating in the temperature range of 25–80 °C.

Considering the simplicity of the approach and the fact that an improvement of just one order of magnitude in proton conductivity could have a dramatic effect on the performance of industrial devices,<sup>25</sup> new materials based on this concept could eventually replace today's standard perfluorinated polymers. A promising strategy to achieve this goal lies in the

manipulation of channel size and density combined with the synthetic versatility of SI-ATRP to grow a plethora of different monomers. The monomer used in the present study contains ester linkages, which might not be the most suitable ones for different industrial applications. Even though, our results obtained at different temperatures after soaking the PEL brush in highly acidic solutions (0.1 N HCl) indicate that poly(3-sulfopropylmethacrylate) brushes are robust enough to attain stable and reproducible proton conductivity values. Future strategies to improve the robustness of the brush layer under more extreme conditions may include the use of more robust polymers with fully acid-stable linkages, like ether. It is worth noting that the goal of these proof-of-concept experiments is to provide a framework for future development in the PEM research field, where perfluorinated polymers, with their economical and environmental impacts, are still the materials of choice.

## Conclusions

These results describe the use of highly ordered macroporous silicon modified with polyelectrolyte brushes as a promising alternative for producing tailorable, robust and self-standing proton conducting membranes. This very simple and straightforward strategy allows for the generation of artificial proton conducting channels, as demonstrated by proton conductivity values of  $\sim 10^{-2}$  S/cm. Considering the versatile chemical nature of ATRP and the wide diversity of macroporous silicon architectures that can be fabricated, we believe that this approach constitutes a benchmark for the preparation and study of model proton conducting systems and, furthermore, for the large-scale fabrication of membranes suitable for different industrial applications.

**Acknowledgment.** B.Y. acknowledges support from the Higher Education Commission (HEC) of Pakistan and Deutscher Akademischer Austauschdienst (DAAD) (Code #A/04/30795). O.A. is a CONICET member and acknowledges financial support from the Max Planck Society (Germany), the Alexander von Humboldt Stiftung (Germany) and the Centro Interdisciplinario de Nanociencia y Nanotecnología (CINN) (IP-PAE, ANPCyT - Argentina). We thank Dr. B. Mathias and S. Ouardi (University of Mainz, Germany) for AAS and XPS analysis. We are also grateful to Gunnar Glasser for helpful assistance in SEM imaging.

JA804683J

- (23) Tredgold, R. H. *Order in Thin Organic Films*; Cambridge University Press: Cambridge, 1994; Chapter 6, p 120.  
 (24) Kluth, G. J.; Sander, M.; Sung, M. M.; Maboudian, R. *J. Vac. Sci. Technol. A* **1998**, *16*, 932.  
 (25) Haile, S. M.; Boysen, D. A.; Chisholm, C. R. I.; Merle, R. B. *Nature* **2001**, *410*, 910–913.